frontiers | Frontiers in Astronomy and Space Sciences

TYPE Original Research
PUBLISHED 06 February 2026
DOI 10.3389/fspas.2025.1720301

OPEN ACCESS

EDITED BY
Michael Zemcov,
Rochester Institute of Technology (RIT),
United States

REVIEWED BY
Kamsali Nagaraja,
Bangalore University, India
Ramazan ATICI,
Mus Alparslan University, Türkiye

*CORRESPONDENCE
Maris Usis,
mau13@case.edu

†PRESENT ADDRESS
Adam Goodman
Space Exploration Technologies Corporation (SpaceX) Hawthorne,
United States

RECEIVED 07 October 2025
REVISED 27 December 2025
ACCEPTED 29 December 2025
PUBLISHED 06 February 2026

CITATION
Usis M, Goodman A, Schwartz L, Kazdan D, Collins K, Gibbons J, Sastry S, Ayres L, Brault C, Byas S, Dompke M, Dowell M, Eggert R, Erdag A, Ervin J, Goodwin D, Nelson S, Nichols S, Tulgetske O and Zorman C (2026) Detecting changes in along-path HF propagation during the April 2024 total solar eclipse with radio amateurs and low-cost instrumentation. *Front. Astron. Space Sci.* 12:1720301. doi: 10.3389/fspas.2025.1720301

Detecting changes in along-path HF propagation during the April 2024 total solar eclipse with radio amateurs and low-cost instrumentation

Maris Usis[1]*, Adam Goodman[1†], Laura Schwartz[1,2], David Kazdan[1], Kristina Collins[1,3], John Gibbons[1], Shashank Sastry[1], Lucy Ayres[4], Christopher Brault[5], Seth Byas[6], Michael Dompke[7], Michelle Dowell[4], Rowan Eggert[6], Aras Erdag[4], James Ervin[7], Dave Goodwin[8], Scarlett Nelson[5], Stephen Nichols[5], Olivia Tulgetske[5] and Christian Zorman[1]

[1]Electrical, Computer and Systems Engineering Department, Case Western Reserve University, Cleveland, OH, United States, [2]Oxford University, Oxford, United Kingdom, [3]Space Science Institute, Boulder, CO, United States, [4]Episcopal Collegiate School, Little Rock, AR, United States, [5]Saint Louis University, Saint Louis, MO, United States, [6]Indiana State University, Terre Haute, IN, United States, [7]Texas A&M University, College Station, TX, United States, [8]Radio Amateurs of Canada, Ottawa, ON, Canada

The total solar eclipse of April 8, 2024 presented a uniquely favorable circumstance for radio science. The Moon's shadow passed near Canadian time standard station CHU, which transmits in the high frequency (HF, *i.e.*, 3–30 MHz) band. It was therefore possible to observe signal changes due to shifting ionospheric conditions along the path of the eclipse by using CHU as a signal of opportunity. In under 3 months, our undergraduate team developed and deployed low-cost instrumentation to record CHU for timing and amplitude analysis. 18 units were distributed across 6 locations roughly aligned with the eclipse path. Each unit contained a radio recorder which retained time traceability to UTC via GPS time synchronization, allowing capture of the CHU signal with no unbounded error beyond the 50 µs sampling interval. Seven units captured changes in the received signal during the eclipse, most notably a tenfold increase in the signal strength at 7.85 MHz for a unit in Little Rock, AR. Its timing suggests a one-hop propagation path reflecting in the ionosphere over Cleveland, OH. The stations were deployed to and maintained by volunteers contacted through the amateur radio and citizen science community. This campaign demonstrates the accessibility and effectiveness of research using low-cost instrumentation and the power of citizen science.

KEYWORDS

CHU, citizen science, distributed sensing, eclipse, ionosphere, multipath, radio, WWV

1 Introduction

Solar eclipses present a rare approximation of a controlled experiment in space: They constitute a known period of time in which photoionization is depressed

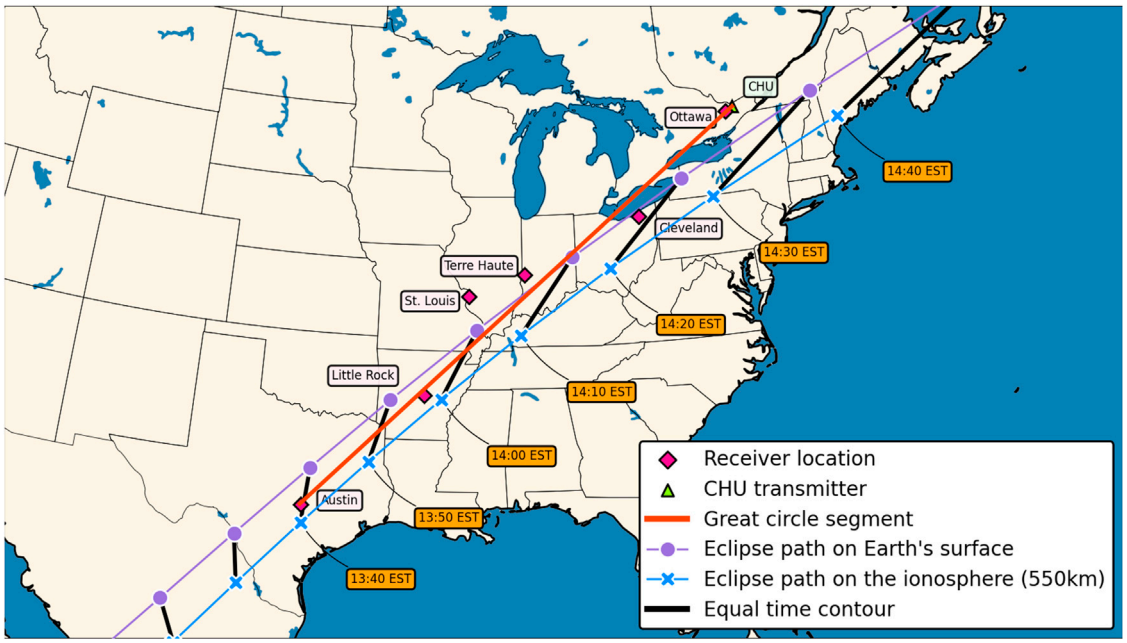

FIGURE 1
Map showing the geography of the experiment. Receiver locations, transmitter location, and the eclipse path are marked.

in a particular region of the Earth, independent of other factors impacting the space weather environment. Capitalizing on this opportunity generally requires distributed instrumentation campaigns, with optimal instrument placement determined by the path of totality. For this reason, solar eclipses have historically been rich moments for crowdsourced data collection and citizen science (Munn, 1924; Lane and Walsh, 1925; Meisel et al., 1976; Frissell et al., 2018; Collins, 2020; Collins et al., 2021a; Collins et al., 2022). In recent years the increasing availability of low-cost instrumentation—including single-board computers, GPS-disciplined oscillators and open-source hardware projects—has made these campaigns easier to conduct.

The total solar eclipse of April 8, 2024 presented a unique opportunity for radio science. The National Research Council Canada time-standard radio station CHU is in Ottawa, Ontario, close to the path of the eclipse's totality. Radio signals propagating along the Earth's surface trace a great circle path, formed by drawing a line passing through two points on a sphere. Such a path, traced from CHU to Austin, approximates the April 2024 eclipse path, as shown in Figure 1. Eclipse experiments often assess propagation paths across the path of totality; this eclipse's geometry facilitated an investigation of *along-path* signal propagation. We hypothesized that sequential measurements of signal strength and time-of-flight during an eclipse path traversal could be used to compute the number of radio "hops" along the path, as well as to assess ion recombination time in the ionosphere. This paper presents a review of the data collection process and related citizen science concerns.

The following research goals were established:

1. Develop a low-cost system to record CHU signal transmissions.
2. Validate the system's precision and accuracy in measuring the broadcast signal from CHU.
3. Deploy the system to citizen scientist volunteers along the path of totality.
4. Determine whether the system detected changes in signal propagation patterns during the eclipse.
5. Make publicly available a dataset for studying eclipse effects on radio propagation and the ionosphere.

2 Science background

The ionosphere is the conducting region of Earth's upper atmosphere that extends from approximately 50–1000 km above the surface (Esmaeili-Karnawah et al., 2024; Poole, 1999; Radicella and Migoya-Orué, 2021). Extreme Ultraviolet (EUV) and X-ray radiation from the sun interact with gases at these altitudes, ionizing them and creating free electrons which form a plasma. This plasma enables long-distance high-frequency radio transmission by reflecting radio waves back to Earth. Interactions between this plasma and radio waves depend primarily on neutral particle density for absorption and electron density for refraction. These properties vary across altitudes, but are stratified into four distinct layers of ionization: D, E, F1, and F2. Radio propagation characteristics manifest short and long term variations in signal strength, time of flight, and Doppler shift (Cameron et al., 2021). Over a short time span, the most significant changes are diel (day/night) variations caused by photoionization.

3 Methodology

The eclipse campaign used two types of stations: "EQ" stations, which comprised volunteered hardware that recorded. WAV files of CHU, and "ET" stations, which were specifically constructed and deployed for along-path measurement. This paper focuses on the latter.

3.1 Station architecture

The Eclipse Tracking (ET) unit is a system designed to record the 1 kHz signal tones from the Canadian time-standard radio station CHU. It serves as a GPS-triggered recording device that captures the demodulated audio of the CHU signal. Each device performs these critical functions:

- GPS synchronization: At the start of each UTC second, marked by a GPS 1PPS (one pulse per second) signal, a microcontroller begins sampling the received audio signal. Since the CHU second tick also begins at the start of each second, this allows for time-of-flight measurements.
- Signal reception: A radio receiver is provided with the unit to receive the CHU signal for the desired time period.
- Sampling: The audio signal is sampled at a high enough sample rate to capture the 1 kHz signal tones without aliasing and allow for delay measurements.
- Data processing and storage: The ET unit processes the captured signal, adding GPS timing and location metadata and storing the data in a CSV file. The data is then uploaded to a remote server for redundancy and compressed locally to reduce storage requirements.
- Remote monitoring and access: Where internet connection is available, the unit is accessible remotely through a peer-to-peer VPN connection. This allows experiment administrators to configure the ET units remotely in the event of user error. A monitoring dashboard also takes advantage of this remote access, and gives a quick overview of system status through a webpage.

Figure 2 shows a high-level block diagram of the system, describing the flow of information through each component. The start block represents the XHDATA radio receiver. The XHDATA receiver is connected to an audio front-end circuit on the ET unit. This circuit includes a 3.95 kHz low-pass filter and a 267 Hz high-pass filter to isolate the 1 kHz signal. This audio signal is then sampled every second by a microcontroller, triggered by a 1PPS rising edge from the GPS module. This microcontroller also receives data every second from the GPS module which provides a UTC timestamp. Once the signal is sampled, it, along with relevant information from the GPS module, is sent to the Raspberry Pi 4 over a serial port. Table 1 shows the bill of materials for the ET unit, which was designed to be as low-cost as possible while still meeting the requirements of the experiment. The total cost of each unit was approximately $100.

Figure 3 shows an assembled ET unit. All ET units were assembled and tested before deployment. This protocol included powering on a unit, verifying a signal was displayed on the dashboard, and verifying that the onboard indicators showed successful operation. Due to the rapid development timeline and limited resources, comprehensive validation before deployment was not possible, so the validation was performed *post hoc*. In this more comprehensive validation process, function generators were used to simulate CHU's signal at each frequency. Three ET units were evaluated over a 2-week period. Figure 4 depicts a block diagram of this validation setup. Analysis of the data showed no drift in timing or amplitude measurements during the validation period. Validation results are provided by (Usis, 2025, Chapter 3).

The software also provided remote access to live data and metrics for each deployed unit using a website serving a JSON[1] representation of the latest data. A centralized server would aggregate the data from many devices in real-time onto a publicly viewable dashboard. A screenshot of the dashboard is shown in Figure 5. Each graph on the dashboard displays a second-tick capture from a single unit. Green indicates a functional unit, yellow indicates GPS loss, and red indicates an error. This information enabled debugging data collection issues in real-time.

3.2 Citizen science deployment

It was financially and logistically infeasible to send a team of researchers to each location. Instead, the ET units were designed to be shipped to a given location and set up by volunteer maintainers. Station maintainers were recruited through the American Radio Relay League's Collegiate Amateur Radio Program, interest groups for eclipse enthusiasts, and personal connections. They were chosen to host ET units based on their location and proximity along the eclipse path, roughly evenly spaced between Austin, Texas and CHU. A sixth station was placed near the investigators' location on the Case Western Reserve University satellite campus at Squire Valleevue Farm, also on the eclipse path.

Monitoring/recording stations were placed at the following locations:

Figure 1 is a map showing the locations of ET unit deployments, along with the eclipse path and transmitter location. The Ottawa, Ontario location was chosen as a control location intended to receive the CHU transmission through line-of-sight propagation rather than the ionosphere. It was located within 50 km of the CHU transmitter.

The volunteer maintainers were given three ET units each as described in Section 3.1. The only equipment the volunteers needed to provide were a mouse and keyboard to interface with the system for configuration, a USB adapter to fully charge the radio batteries, and a screwdriver to ensure the power supply and audio cable were properly attached. The volunteer maintainers received a set of instructions (Goodman et al., 2024b) on how to configure the units for the experiment. Notable components of the installation protocol include:

- Placing GPS antennas near windows or outdoors for the best satellite reception.

1 JavaScript Object Notation.

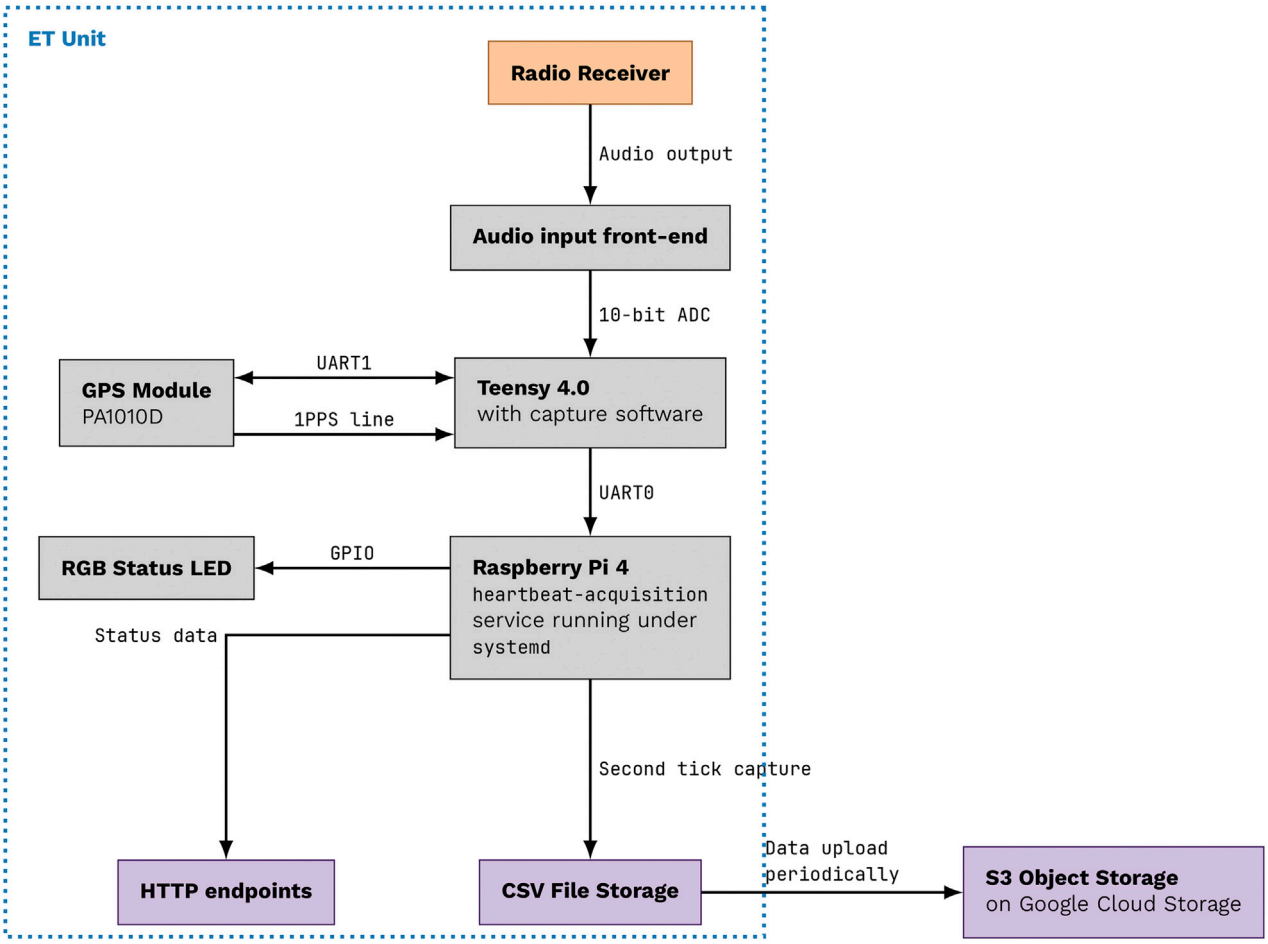

FIGURE 2
High-level block diagram of the ET unit.

TABLE 1 Bill of materials for the ET unit.

Component	Purpose
Raspberry Pi 4	Computer for data processing and storage
Teensy 4.0	Microcontroller for signal sampling and processing
PA1010D	GPS receiver for time synchronization
XHDATA D-109WB	HF radio receiver for signal reception
EFU120200F2000	12 V linear power supply
Custom PCB	Custom PCB connecting all components and distributing power, shown as part of the unit in Figure 3 and documented in Usis (2025)
Antenna	Length of wire to be used as antenna with a terminal block connector compatible with the radio
500 GB hard drive	External storage used for data redundancy and recovery

- Deploying the wire antennas vertically to match the polarization of the CHU signal (Figure 6).
- Connecting the power supply to the ET board before plugging it into the receptacle. This was a critical step, as the sensitive switch-mode power supply IC could be potentially detonated as a result of lead inductance if the power supply was connected to the receptacle first.
- Connecting the ET units to internet for remote access and monitoring.
- Setting the radio volume to the maximum level possible without clipping (as shown by the red LED on the PCB).
- Fully charging the radio batteries before the unit is powered on to prevent drawing too much current from the Raspberry Pi USB ports.

Stations connected to the internet uploaded live data in addition to logging all data to their hard drives. At the conclusion of the experiment period, all participants returned the physical hard drives to the investigators.

The deployed network of ET units were set to record data from 1 week before through 1 week after the eclipse. The exact timeline ran from April 1, 2024 UTC through April 15, 2024 UTC. This plan provided 2 weeks of data to establish a baseline prior to and following the eclipse event, enabling the ability to discern between

TABLE 2 Deployment locations for the ET units.

Location	ET units (3.3, 7.85, 14.67 MHz)	Latitude	Longitude
Ottawa, Ontario, Canada	1007, 1004, 1008	45.14	−76.16
Cleveland, Ohio, United States	1016, 0002, 0001	41.49	−81.42
Saint Louis, Missouri, United States	1014, 1001, 1015	38.62	−90.19
Terre Haute, Indiana, United States	1002, 1012, 1010	39.47	−87.40
Little Rock, Arkansas, United States	1006, 1003, 1009	34.75	−92.29
Austin, Texas, United States	1013, 1011, 1005	30.25	−97.68

FIGURE 3
Assembled ET unit. The left block is a Raspberry Pi with the custom PCB (purple) as a daughterboard ("hat"). The small green board is the Teensy 4.0, and the blue board is the GPS receiver, which has a trailing SMA connector that will be connected to a GPS antenna. The custom PCB includes an indicator LED to provide station status information for maintainers. The two wires in a terminal block on the short side of the board connect to the audio output of the HF receiver (bottom). The two wires in a terminal block on the long side of the board connect to a 12V power supply. One of the two USB cables on the right side of the board connects to the hard drive (bottom of picture) and the other provides 5V power to the HF receiver.

changes as a result of the eclipse and normal variations in signal reception at each location.

3.3 Data analysis

The audio of the radio receiver was sampled every second for a duration of 360 ms. This duration was chosen to ensure that both the 300 ms tone and any delays were captured. A 20 kHz sample rate was used, resulting in a precision of 50 µs for each individual sample. Thus, each second capture is 7200 samples in duration. A unit running for the duration of the experiment without error would have collected a $12\,96\,000 \times 7200$ dataset (3600 s/hr · 24 h/d · 15 days = 12 96 000 samples on the time-of-day axis). Because the samples were limited to 0 to 1023, 16-bit integers (a.k.a. *short int*) were used to reduce storage size. During analysis, the integers are converted to floating-point values by normalizing the range of values [01,023] to [−1, 1].

Visualization of the time-series data was crucial to development and validation of the devices and analysis of the data. One method used is shown in Figure 7. Each second capture is represented as a row of pixels, with the x-coordinate representing sample time (*i.e.* the time within the capture). The amplitude of each sample in the signal is represented by the color of the pixel. To visualize changes in the signal over time, these rasterized captures can be stacked across the capture time dimension, resulting in a waterfall plot (Figure 8).

The waterfall plot provides a good visual overview of the data, and anomalies or changes in signal strength can be assessed visually. However, to extract numerical values for signal delay and amplitude, a more precise method is required. This can be achieved using cross-correlation, which is defined as the similarity between two signals as a function of time-lag. Figure 9 shows an illustration of this process. The red signal, $x[t]$, represents the ideal signal, starting at time $t = 0$ with no delay. The blue signal, $y[t]$, represents the field data, containing the ideal signal delayed by an unknown amount of time t_{delay}. The cross-correlation is calculated by multiplying the two signals together at different time delays of $x[t]$, the ideal signal. The result is a new signal, $z[t]$, which represents the similarity between the two signals at each time delay. The maximum value of $z[t]$ indicates the time-lag at which the two signals are most similar. In this case, the maximum value occurs at $t_{\text{delay}} = 0.8$ s, indicating that the ideal signal is present in the field data with a delay of 0.8 s.

Mathematically, the discrete-time cross-correlation between signals x and y is defined as:

$$(x \star y)[t] = \sum_{n=-\infty}^{\infty} x[n]\, y[n+t] \tag{1}$$

The time delay, t_{delay}, can be calculated by finding the time at which the cross-correlation is maximized:

$$t_{\text{delay}} = \arg\max_{t \in \mathbb{Z}} (x \star y)[t] \tag{2}$$

The template used in this analysis consisted of 300 ms of a pure 1 kHz sine wave sampled at 20 kHz, representing an ideal CHU signal. We cross-correlated this template with each second-tick capture (7200 samples) using the `scipy.signal.correlate` function with mode set to "same", yielding an output of 7200 samples aligned to the original capture. To quantify received signal strength, we extracted the peak magnitude of each cross-correlation result:

$$S[t] = \max_{t \in \mathbb{Z}} (x \star y)[t] \tag{3}$$

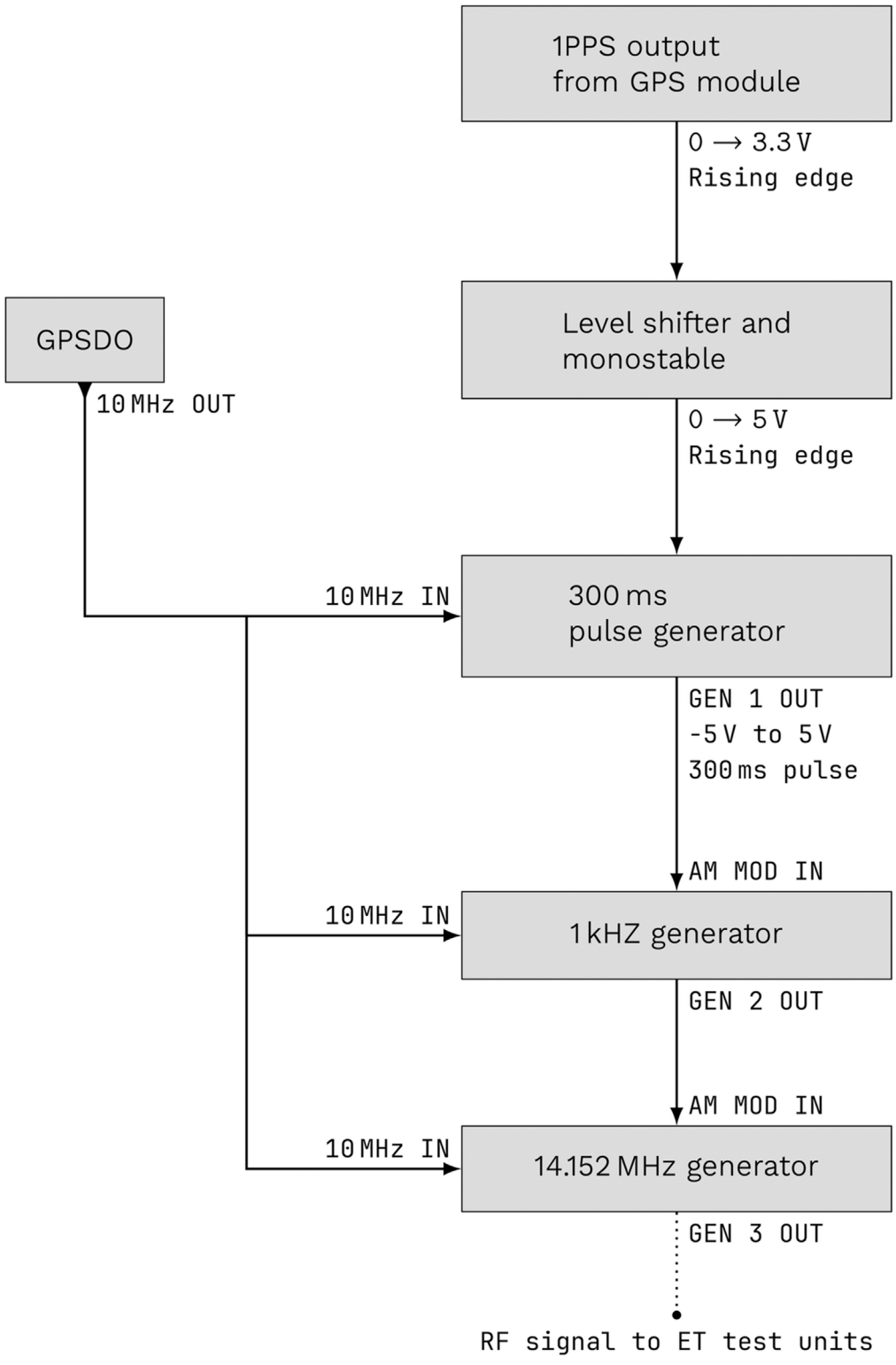

FIGURE 4
This illustrates how the simulated CHU signal is generated during system validation.

where $x \star y$ denotes the cross-correlation between the template and the captured signal.

The raw data contained gaps due to runtime errors, so we applied linear interpolation to produce a complete set of 86 400 samples per day. We then applied a 60 s moving average filter to reduce noise, downsampling the data to 1440 relative signal strength measurements per day. These processed values formed the basis for the subsequent analysis.

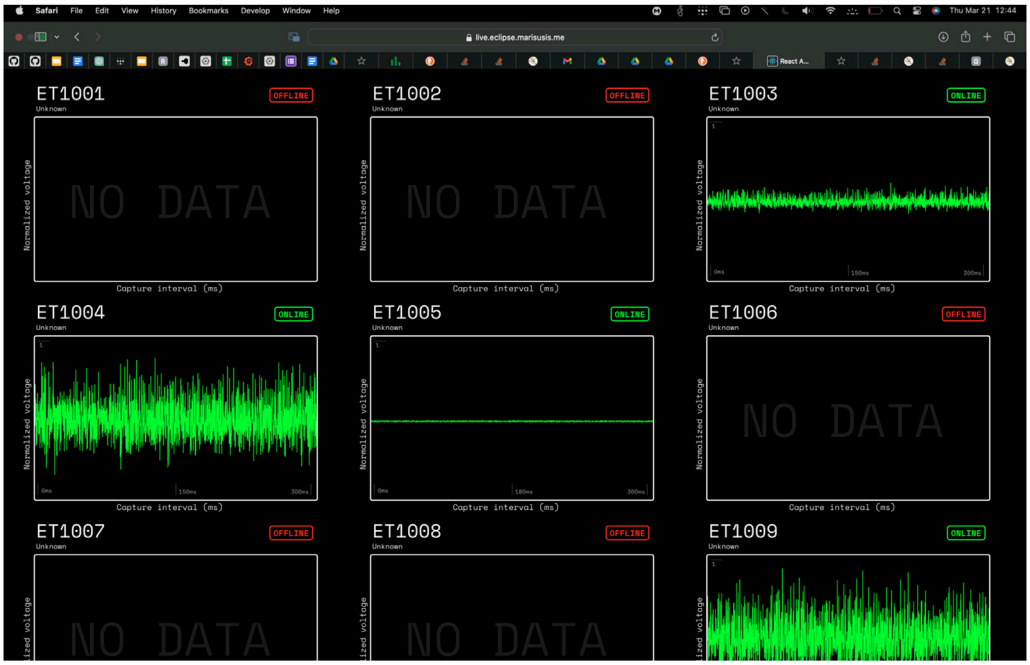

FIGURE 5
Screenshot of the web dashboard built for remote, real-time monitoring of the ET unit data collection.

FIGURE 6
Antenna setups at CWRU and Little Rock stations.

4 Results

4.1 Summary

The April 8, 2024 eclipse experiment generated approximately 2 TB of time-series data collected from 19 ET units deployed across six locations along the eclipse path. Each unit operated continuously for approximately 2 weeks, capturing CHU signals at 1-s intervals to establish baseline propagation characteristics and detect eclipse-induced anomalies.

Station failures and outages did occur: as shown in Figure 10, only 1 of these units in Little Rock, AK monitoring 7.85 MHz, collected data for the entire experiment. 16 out of 19 units recorded data during the eclipse, and in most cases a day's worth of data is available before, during, and after the eclipse for the purposes of comparison.

The primary analytical approach focuses on identifying deviations from normal diel propagation patterns. Over the 2-week experiment duration, the planetary K_p remained below 4 (NOAA Space Weather Prediction Center, 2024). Thus, we assumed patterns in propagation and signal strength would be primarily driven by the day-night cycle rather than eruptive solar phenomena. Figure 11 shows a plot of the planetary K_p value. This approach accounts for location-specific ionospheric conditions, equipment variations, and the unique geometry of each signal path between CHU and the receiving stations (Cameron et al., 2021).

Data that show consistent patterns in signal strength indicate normal propagation behavior, while inconsistent patterns suggest anomalous conditions. This approach is more robust than assuming theoretical day/night propagation models because it accounts for location-specific ionospheric conditions, equipment variations, and the unique geometry of each CHU signal path. As such, each deployed ET unit produced a dataset that can be categorized into one of three groups:

1. Valid with eclipse event: Shows consistent diel patterns and a clear deviation from average behavior during the eclipse, referred to as an eclipse event;
2. Valid without eclipse event: Shows consistent diel patterns but no detectable eclipse event;
3. Invalid/inoperative: Shows inconsistent patterns or failed to collect data due to hardware or maintainer issues.

In this context, the average diel propagation pattern (or "average behavior") is defined as the baseline 24-h signal strength profile, obtained by taking the mean signal value at each time point across all non-eclipse days. Our null hypothesis (H_0) is that the

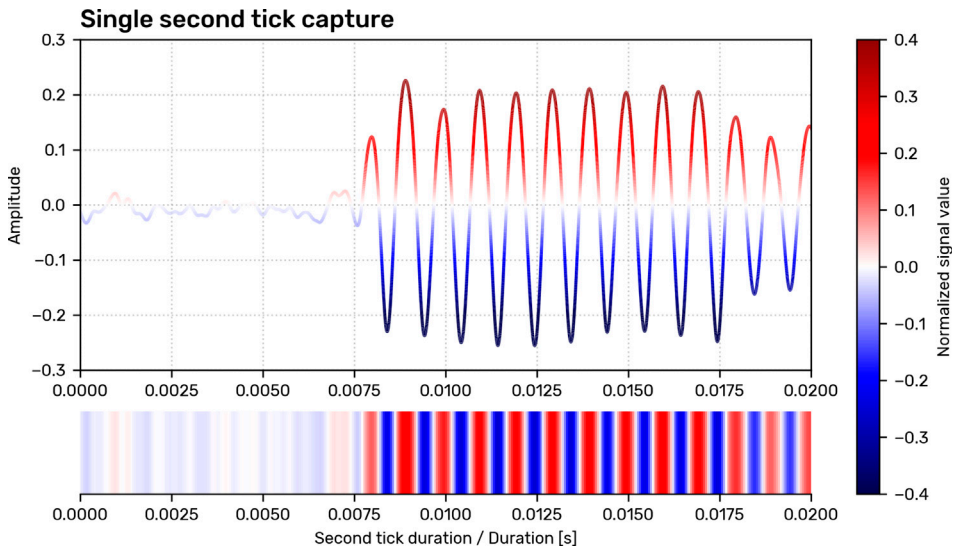

FIGURE 7
An image showing the process of transforming a recorded signal into a waterfall plot for visualization. The amplitude is mapped to color, as shown.

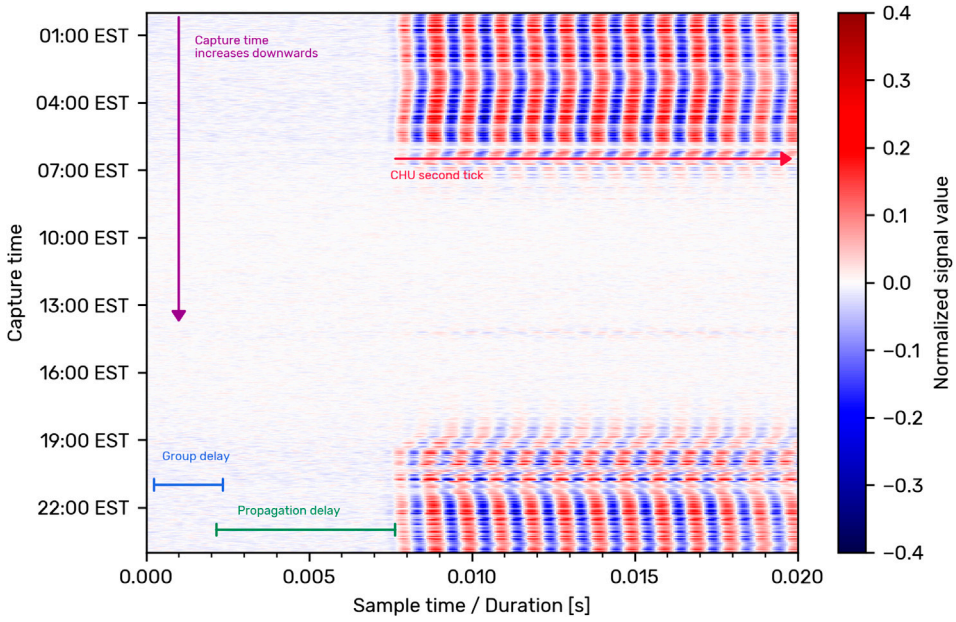

FIGURE 8
A complete waterfall plot with annotations. The vertical axis represents *capture time* (*i.e.* the time when the 1PPS triggered the start of a capture). The capture time starts at the top, and increases going to the bottom of the graph, as indicated by the purple arrow on the left. The horizontal axis represents sample time (*i.e.*, for a given capture, a pixel at a given x-coordinate represents its position in the capture). The color of each pixel represents its amplitude. A colorbar on the right side of the graph indicates the values corresponding to each pixel color. We used divergent color maps to indicate both positive and negative values.

distribution of signal reception on eclipse days is not different than the signal reception on non-eclipse days—our equipment did not detect a change in signal reception as a result of the eclipse. Using a permutation test, we estimate the probability of sampling certain behavior assuming the null hypothesis is true. Figure 12 shows the results of a permutation test performed on data from the Little Rock, AR ET unit on 7.85 MHz. As indicated by the purple strip in the figure, there is a peak in signal reception and accompanying p-values that fall below our chosen level of significance. We can then reject the null hypothesis for those values and say they are statistically significant—an eclipse event was detected. A confidence interval generated using bootstrapping with $B = 20000$ on the sample distribution is also shown in the bottom plot.

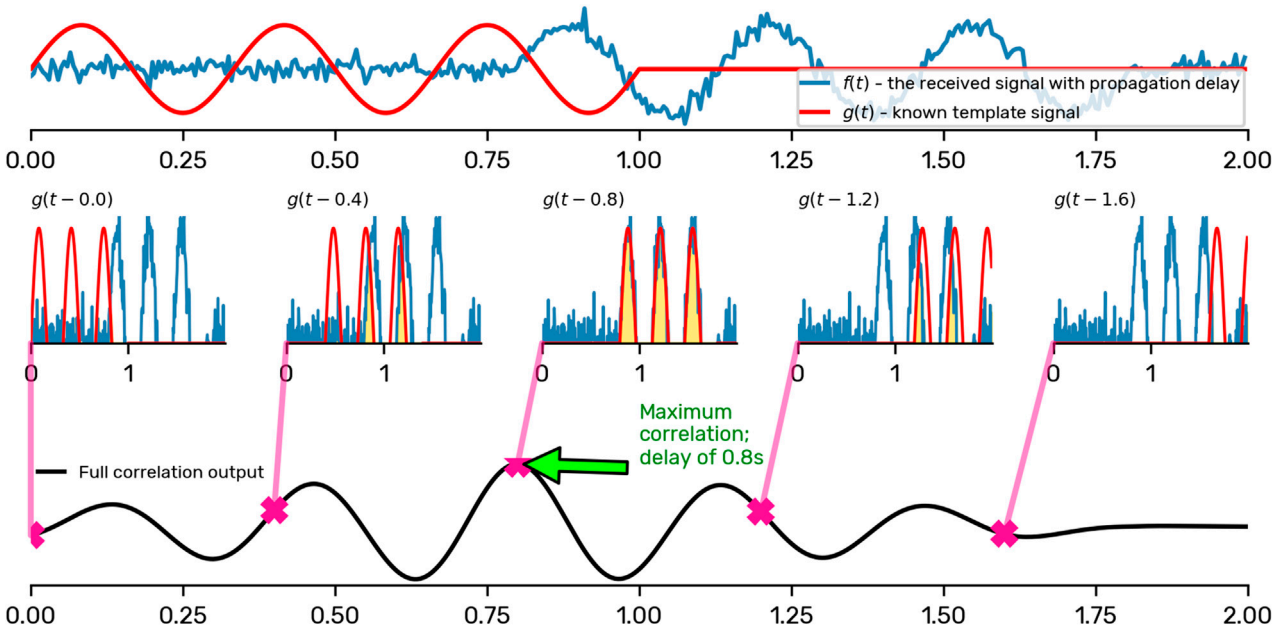

FIGURE 9
An illustration of the cross-correlation process Equations 1–3.

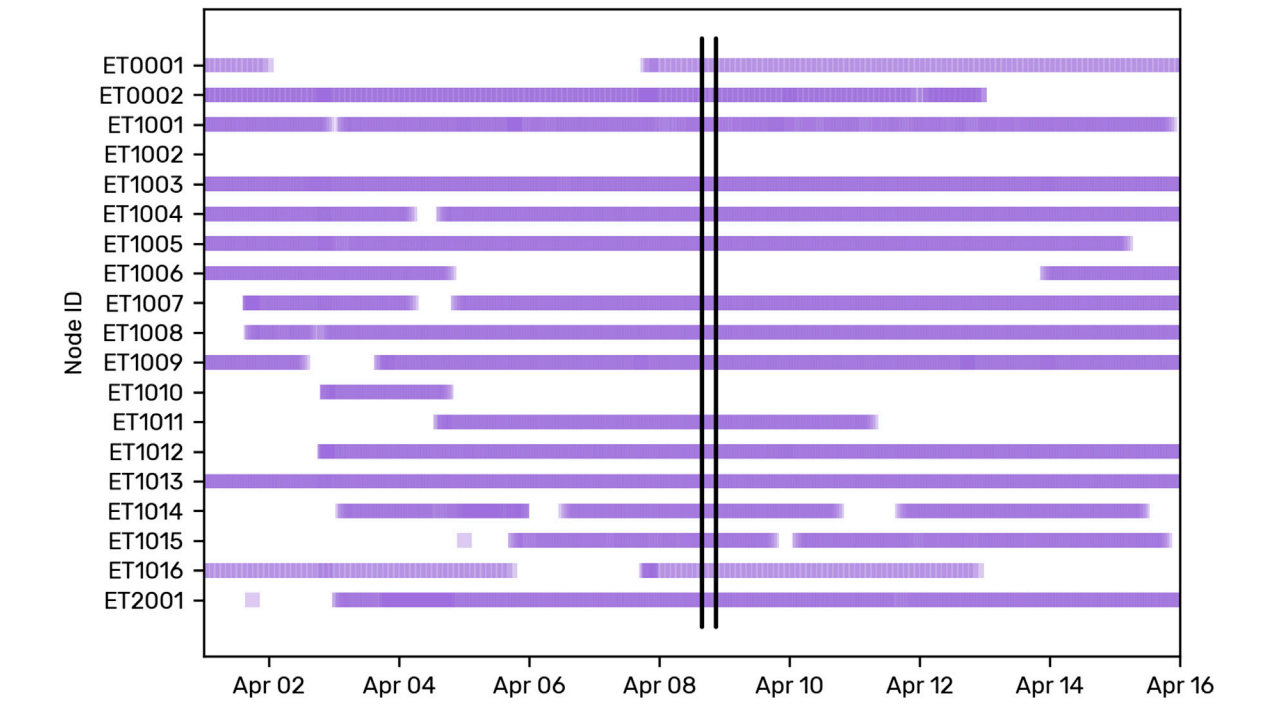

FIGURE 10
Data availability across all ET units for this experiment. Locations and frequencies for each unit are listed in Table 2.

Of the 19 deployed units, 14 produced valid datasets. Of these 14 valid units, 6 showed eclipse events within our chosen level of significance, while 8 showed normal diel patterns without meeting the stated criteria for an eclipse event. The remaining 5 units were classified as invalid or inoperative.

Figure 13 shows examples of the three data categories. The black line represents signal strength throughout the day of the eclipse. The

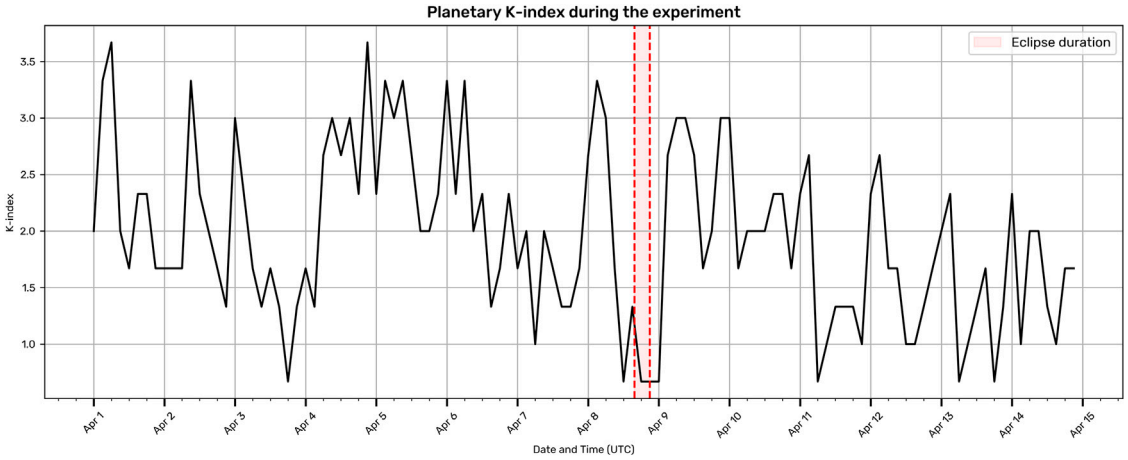

FIGURE 11
A graph of the planetary K-value for the duration of the experiment, with the time of the eclipse highlighted. No geomagnetic storms occurred during the experiment period. Data provided by NOAA Space Weather Prediction Center (SWPC) NOAA Space Weather Prediction Center (2024).

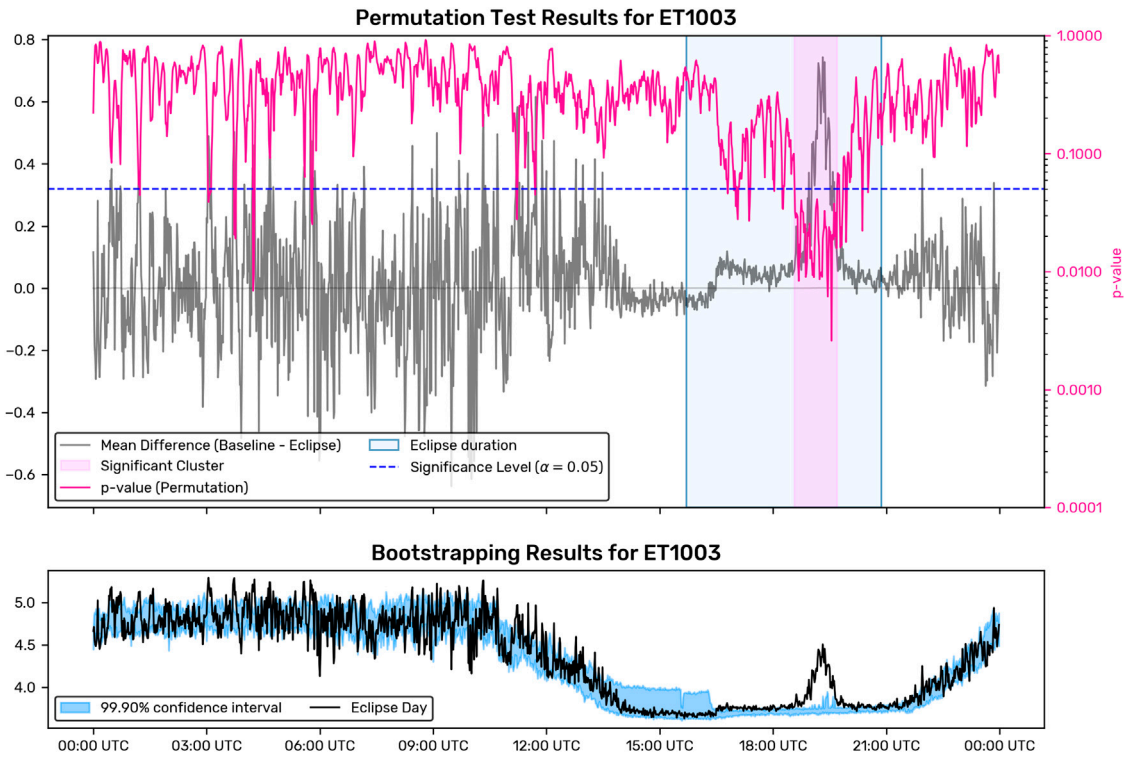

FIGURE 12
Permutation test and boostrap confidence interval results for ET1003 (Little Rock, AR on 7.85 MHz).

red and blue lines are the average signal strength before and after the eclipse, respectively. These averages are shown separately to visualize any changes in the baseline signal behavior that may have persisted after the eclipse event. The top plot shows a valid dataset with a clear diel pattern, but no eclipse event is detected. The middle plot shows a dataset with nearly the same diel pattern; however, an eclipse event is detected. The bottom plot represents a failure: no diel pattern exists on the day of the eclipse.

4.2 Case study of Little Rock, AR data

Figure 14 presents a signal strength plot for data collected by the Episcopal Collegiate School station in Little Rock, AR on 7.85 MHz. The blue and red lines show the average signal strength before and after the eclipse, respectively. The black line shows the signal strength during the eclipse.

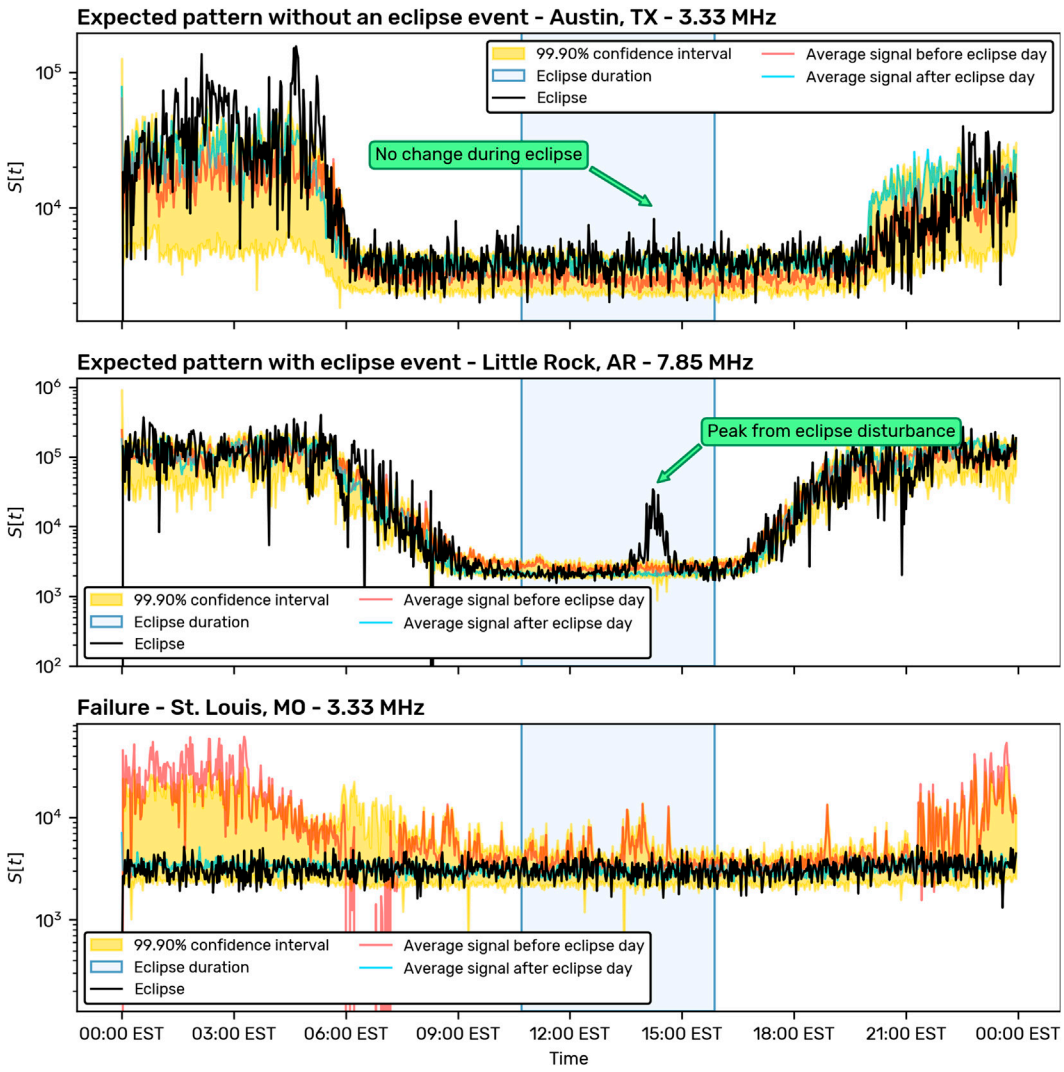

FIGURE 13
These plots illustrate the difference between the three data categories defined in the results. The y-axis shows the output of cross-correlation as shown in Figure 9.

A significant change in signal reception is observed during the eclipse. This is likely a result of the Moon's shadow causing temporary nighttime conditions in the ionosphere, allowing for better propagation of the 7.85 MHz signal. The plots on the left of Figure 14 show an illustration of this effect. The signal strength doesn't quite reach the levels that would be expected for nighttime reception, however, remaining nearly an order of magnitude below control nighttime levels. This is likely due to the short duration of totality at a given location (less than 5 min), preventing the ionosphere from fully forming its nighttime state before solar radiation returns (Espenak, 2014).

The curvature of the Earth's surface and the angle of the Moon's shadow result in a counterintuitive gap between the path of totality on the ground and the path of totality at altitude, an effect which is more pronounced at higher latitudes. Eclipse-related signal impacts relate to the path of the shadow at altitude, not the location of the shadow on Earth's surface. The effect is shown in Figure 15 and visualized over time in Figure 1, where the purple line represents the path of the Moon's shadow on the surface of the Earth and the blue line represents the path of the shadow on the ionosphere. Black lines link the two paths at corresponding time points, illustrating the spatial offset between them.

Using available ephemeris data supplied by the Astropy Python package, the path of the Moon's shadow was calculated and projected onto a plane defined by the positions of Little Rock, CHU, and the Earth's center at 1415 EST/1915 UTC, near when the peak occurred Kerkwijk et al. (2020); Price-Whelan et al. (2022). Figure 15 shows a scale visualization of this. This analysis sets the reflection point at approximately the halfway point between CHU and Little Rock, strongly suggesting a 1-hop propagation path as opposed to a multihop path. This midpoint lies at 39.17°, −84.44°, above Cincinnati, Ohio. Solar obscuration at that point was computed with Frissell (2017) and is overplotted in Figure 16. The peak of the solar obscuration at the midpoint is shown to be concurrent with the peak observed in the received data.

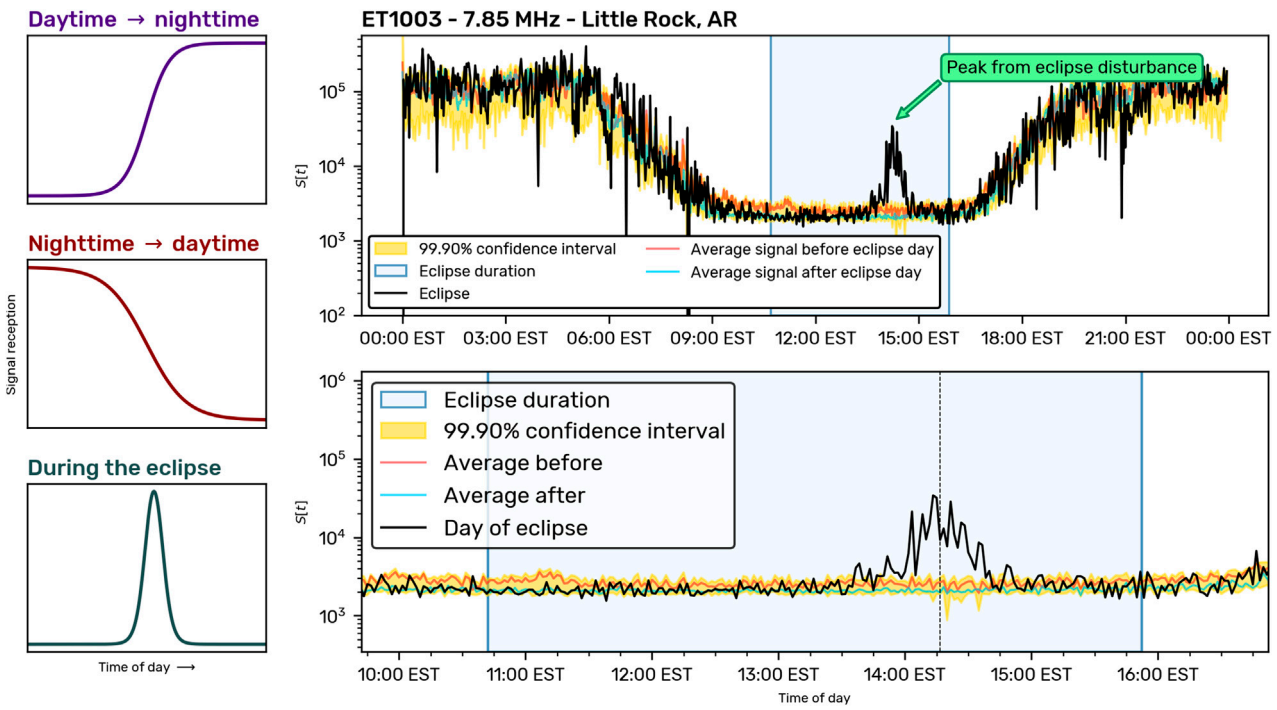

FIGURE 14
Analysis of transmission of CHU 7.85 MHz transmission received in Little Rock, AR during the eclipse, including a zoomed-in view of signal strength.

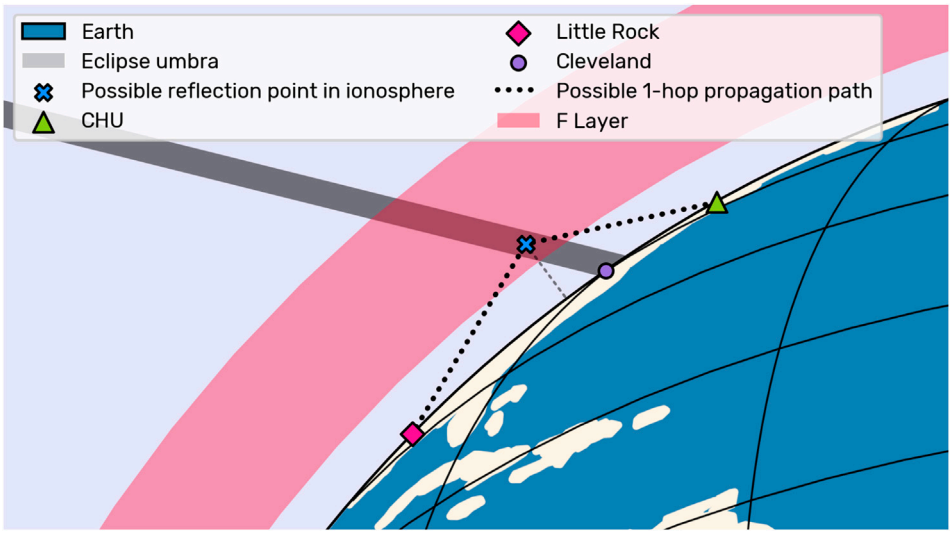

FIGURE 15
Diagram showing the oblique angle of the Moon's shadow on the Earth and the resulting propagation path of the CHU signal at 14:16 EST, during the peak of reception in Little Rock, AR (shown in Figure 14). This figure is to scale and derived from real-world data, except for the size of the shadow (umbra). The height of reflection is approximated at 325 km, the average hmF2 between the Austin and Millstone Hill ionosondes at this time (Reinisch and Galkin, 2011).

Past eclipse studies have shown that reduced photoionization leads to decreased electron density and absorption in the D-region, opening up new HF propagation paths (Zhang et al., 2017). Our observation of signal enhancement is consistent with this pattern. Concurrent ionosonde data is shown in Figure 16. The GIRO ionosondes collect data on a 1 min cadence, and there is no vertical incidence ionosonde at the approximate midpoint between CHU and Little Rock. However, a modest dip in foF2 is observed at Alpena shortly after the Little Rock peak, which is consistent with the eclipse moving south to north.

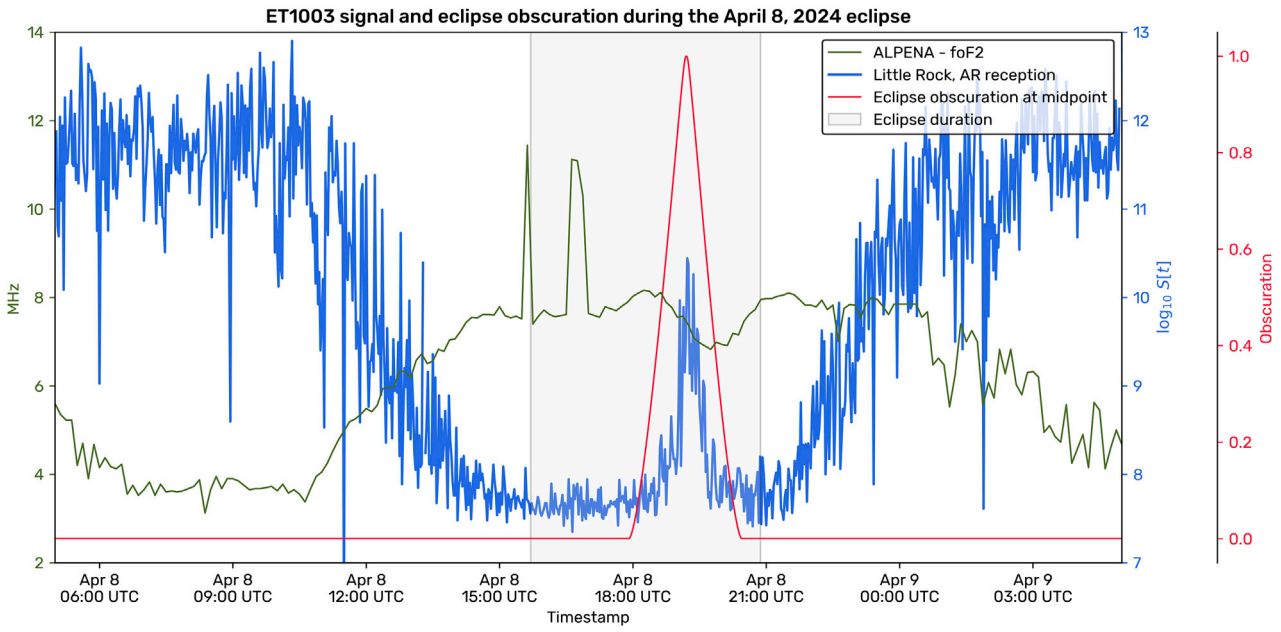

FIGURE 16
Data from the Little Rock station, including the period shown in Figure 14, is overplotted with eclipse obscuration data for the midpoint shown in Figure 15 and foF2 data from the GIRO ionosonde (Reinisch and Galkin, 2011) at Alpena, MI. The Alpena ionosonde, which is west of the eclipse path but is the nearest ionosonde to the midpoint between CHU and Little Rock, shows a dip in foF2 shortly after, consistent with the path of totality moving south to north.

5 Discussion

Due to the nature of the project, not all stations were successful in collecting data. However, by deploying quickly and at scale, we still collected meaningful results despite a tight budget and timeframe.

While the system was low-cost and portable, there were some drawbacks: First, the fact that volunteer maintainers cannot be fully trained to debug stations onsite diminished station reliability, compared to onsite deployment of a trained operator (Usis, 2024, *e.g.*). Second, the units are designed specifically for demodulating and timing 1 kHz tones, limiting their use with other radio beacons. However, the open-source and low-cost approach allows for the deployment and usage of these devices by citizen scientists to support a larger measurement network than would otherwise be possible (Collins, 2023).

In the future, issues related to data quality in a similar project could be avoided by producing a user interface that could fully provide feedback on how to troubleshoot the unit without an internet connection. This would make them easier to operate and enable units to be placed in remote locations that do not have a connection. Using more commercial off-the-shelf (COTS) hardware would also improve ease of procurement and assembly.

Data was originally stored in. CSV format, but converted to HDF5 after collection and uploaded to Zenodo (Goodman 2024a). This design decision was initially motivated by a desire for simplicity, but the resulting files were large and difficult to work with. In the future, this data would be better stored as HDF5-compatible files from the beginning of the experiment. The datasets were manually collated and uploaded to Zenodo, a task which took a significant amount of time for the core team to accomplish. More recent HamSCI experiments such as the Meteor Scatter QSO Party encourage citizen scientists to upload their own datasets in a standardized format to the HamSCI Zenodo community for review by a central science team, which is a much more efficient and scalable protocol.

6 Conclusion

Our citizen science approach allowed resources to be distributed quickly at scale and at a geographic diversity given the limited timeframe and budget. This enabled meaningful data collection and results for the entire project even when some stations failed to produce the required data. An added benefit of crowd sourcing volunteers is that it inspired members of the public and community who may not otherwise engage with ionospheric sciences to take an active role in the experiment and educate themselves and others. Our volunteers included high school students who were previously unfamiliar with amateur radio and how to set up a receiving station, and the publicity of the project promoted amateur radio and ionospheric research on a national level (Nanda and Treseler, 2024). Some lessons of this project can be extended to future citizen science experiments and generalized beyond heliophysics to wider domains of Earth system science.

6.1 Campaign planning

A solar eclipse is a compelling event, and mandates a focused timeline for experiments. Multi-instrument campaigns in Earth system science are often effectively organized through having a strictly defined timeline, even an arbitrary one: the

International Geophysical Year (Lyubovtseva et al., 2020), and the system of International Polar Years of which it is part (National Research Council, 2012), are a testament to the efficacy of this approach. The philosophy of these campaigns is especially timely in today's landscape, when frontier questions often require multiple concurrent measurements from different types of instruments and barriers to entry have been lessened by inexpensive single-board computers and open source hardware.

This project shows that a short timeline is not necessarily counterproductive. Focus and autonomy of the core team was key to success. Scientists must be empowered to take risks and quickly adapt to unpredictable changes and opportunities. This is an important metascientific (Ioannidis et al., 2015) consideration with implications for funding structure: a longer funding timeline, greater reporting burden, or lower risk tolerance would have made this work impossible.

6.2 Team science

The science team of this project consisted of a core university-affiliated group and a distributed group of volunteers. The project was led by an undergraduate team in a senior project class, who received mentorship from faculty and staff; this portion of the project was in a classical mold, although it did also benefit from curricular (Collins et al., 2017) and research integration with the university amateur radio club. The team was able to tap into an existing citizen science community, HamSCI, and reached members of the amateur radio community through multiple methods. The ET stations discussed here were supported by a volunteer group of about 25 individuals, ranging from ninth grade to PhD level. About 50 volunteers recorded audio data (Goodman et al., 2025).

The primary science team maintained an active and positive channel of communication between the core teams and the station maintainers before, during and after the experiment. In recognition for hosting ET units, clubs and individuals were awarded with Ohio buckeye candy and a homemade acrylic plaque in recognition of their contributions (Figure 17). Feedback on the experiment was also shared in the hobbyist literature (Kazdan, 2024), where volunteers were most likely to read articles and to be recognized within their community.

Citizen science is resource-constrained in every aspect except one: personnel. In the classical project management triangle (Project Management Institute, 2004) of time, scope, and resources, this radically extends the latter, presenting new challenges and opportunities for science teams. Crowdsourced measurements have a long history in data collection campaigns (Meehan et al., 2019) and have formed the initial backbone of communication and forecasting networks (Hughes, 2024; McCray, 2021). Today, computer-driven acceleration of crowdsourced data collection is recognized as a transformative advance in observational sciences (Mason et al., 2025). With this acceleration come new obligations to the scientists who recruit and manage these volunteers. Bonney et al. (2009) distinguish between contributory, collaborative, and co-created projects. Boone et al. (2024) identified several traits of successful citizen science leaders, including aligning scientific goals with participatory goals, minimizing barriers to participation, engaging communities, communicating actively with volunteers, integrating training and educational activities, and providing intrinsic and extrinsic rewards to contributors. They noted that successful citizen science leaders cultivate an appreciation of volunteers' contributions and capabilities "characterized by trust, respect and gratitude."

Factors which are often considered challenges to team science can be reframed as advantages in a distributed citizen science context. Team science challenges enumerated by Cooke and Hilton (2015)—high diversity of membership, deep knowledge integration, large size, diversity of goals (referred to as "goal misalignment" in the initial report), permeable boundaries between roles, geographic dispersion, and task interdependence—are all hallmarks of successful citizen science collectives such as HamSCI and Aurorasaurus. Interestingly, these challenges strongly resemble the list of citizen scientists' strengths identified by Ledvina et al. (2023).

Collins et al. (2021b) and Frissell et al. (2023) highlight the harmony between the amateur radio and geospace communities. As the history of amateur radio is closely linked with that of radio science (Yeang, 2013), the distinction between the roles of "amateur radio operator" and "radio scientist" has always been a fluid one, and the two categories often overlap. In this sense, amateur radio is a useful model for Batchelor et al. (2021)'s vision of a flexible STEM workforce in which formal and informal training blend together, and in which citizen science participation can stimulate talent development and interdisciplinary collaboration.

6.3 Instrument design

In the design and deployment of these instruments, numerous design criteria were considered which are common to any distributed instrumentation project with stations maintained by volunteers. The character of such a project may be considered in terms of which of these general criteria are prioritized over one another. As Garvin (1987) notes, some criteria of quality may be mutually reinforcing (durability generally supports reliability, *e.g.*), while others pose tradeoffs. Citizen science decouples some dimensions that are usually coupled: for example, adding additional stations to a citizen science network does not necessarily lead to higher cost. Therefore, citizen science presents a different set of tradeoffs from traditional academic research, and design requirements must be adjusted accordingly.

Some of these considerations include:

- Performance: The capability of stations is dictated by the needs of the science question, and varies widely from project to project. Number, density, and locational distribution of stations should be considered when formulating the science question. Formulation of a science traceability matrix (Weiss et al., 2005) in collaboration with the full citizen science team is highly encouraged in the planning stages of the project.
- Features/Station Agility: In observational science, the performance requirements for a given science question may not be clear until some data has been collected. For example, the first iteration of the HamSCI Personal Space Weather Station, the Grape (Gibbons et al., 2022), successfully gathered a large dataset across dozens of stations

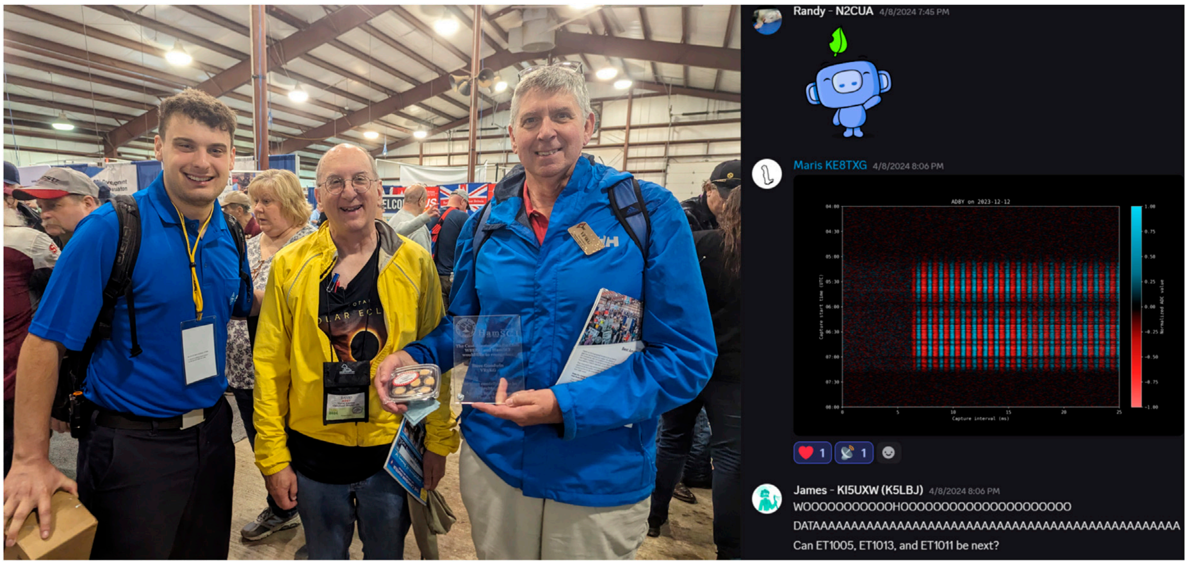

FIGURE 17
Left: Station maintainer Dave Goodwin VE3KG, on right, holding commemorative plaque and complimentary chocolates. Maintainers reported that these small gestures of appreciation meaningfully enhance the citizen science experience by fostering a sense of prestige and participation. Right: Data posted to a team chat for live discussion on the day of the eclipse. Discord was used as an informal communication channel for all team members throughout the campaign, enabling coordination and feedback between volunteer maintainers and the core science team.

(Collins et al., 2023). The analysis of these data prompted questions about multiple carrier signals associated with multiple simultaneous propagation paths, which in turn informed the design requirements of the next PSWS class, the Grape 2 (Gibbons, 2024), which boasted wider spectral recording. Software-defined radios (SDR) are highly agile, but may not be able to supply precise timing or other performance features pertinent to a given science question. However, a network need not be confined to a single methodology: at the time of writing, the PSWS network includes both Grape versions, as well as SDRs.

- Reliability: Is the network capable of collecting data throughout the course of the planned campaign time? Notably, this criterion is reinforced by redundancy in the network, as well as by conformance, durability and serviceability (below).
- Conformance: This criterion includes validation, calibration, and homogeneity of stations across the network. Collins et al. (2022), for example, used a very heterogeneous set of stations to provide an initial proof of concept for the highly consistent system developed in Gibbons et al. (2022).
- Durability: This is desirable for long-term deployments and extreme environments, but in some cases may be readily sacrificed in favor of other criteria.
- Serviceability: This criterion should be considered for both hardware and software. Hardware serviceability includes the incorporation of test points and indicator lamps. Software serviceability is reinforced by remote access and monitoring, such as the live view of station uptime in Figure 5. Designers should also consider whether the instrument should require an internet connection. Ability to restore functionality remotely was extremely useful in this work; the development team could and did access deployed stations via SSH and update software. While remote access to instrument computers is useful, it carries the risk of breaking the network after deployment. Developers should use caution and test code thoroughly on bench hardware before uploading a patch.
- Colocation of Multiple Instruments: Instruments across multiple disciplines can share power and data buses, etc. If the instrument types will not interfere with one another, it's worth considering whether a distributed network or campaign may be usefully integrated with an existing instrument network, or combined with a developing one.

In citizen science projects designed for learning, the quality of the maintainer experience is also an important consideration. National Academies of Sciences and Medicine (2018) distinguish between citizen science designed for learning, citizen science adapted for learning as well as science, and citizen science practices used for the sole purpose of learning which do not yield scientific data. Relevant criteria for instrument design include:

- Station Assembly Procedure: It may be desirable to have the maintainers assemble the stations. For example, the EZIEMag project (Mesquita et al., 2025) distributes station materials in neatly packaged boxes for maintainers to assemble, which enhances the project's capacity for informal education. There is a potential tradeoff here: Pre-assembly of these stations would be very straightforward and could slightly enhance the durability of the stations and the simplicity of the maintainer interface; however, the educational value of the project is important, and the risk of maintainer error is greatly mitigated by the hardware design and thorough documentation.
- Hardware Openness: Pearce (2012) notes the value of replicable science hardware, including the use of commercial

off-the-shelf (COTS) parts and open-source components. The Open Source Hardware Association (OSHWA) defines open source hardware as "hardware whose design is made publicly available so that anyone can study, modify, distribute, make, and sell the design or hardware based on that design." Following this standard often makes hardware cheaper in the long run, and greatly increases serviceability. In projects where volunteers build their own stations, making design information fully available according to open source standards also greatly improves the scalability of the project as a whole. Gibbons et al. (2022) is an example of this approach.

- Data Management Plan: Citizen science projects often result in large data yields which the core science team may not have enough time to analyze. It is highly recommended that data be made compliant with the FAIR (Findable, Accessible, Interoperable, Reusable) standard.
- Maintainer interface: Simplicity, completeness and correctness of the maintainers' interface should be considered. In this experiment, the most important criterion was for the ET stations to be as plug-and-play as possible.

Data availability statement

The datasets presented in this study can be found in online repositories. The names of the repository/repositories and accession number(s) can be found below: https://doi.org/10.5281/zenodo.14257092.

Ethics statement

Written informed consent was obtained from the individual(s) for the publication of any potentially identifiable images or data included in this article.

Author contributions

MU: Writing – original draft, Software, Writing – review and editing, Investigation, Project administration, Formal Analysis, Conceptualization, Methodology, Visualization, Validation, Data curation. AG: Conceptualization, Investigation, Project administration, Funding acquisition, Methodology, Data curation, Writing – original draft, Resources, Writing – review and editing. LS: Formal Analysis, Project administration, Methodology, Data curation, Conceptualization, Writing – original draft, Visualization, Validation, Writing – review and editing, Investigation. DK: Supervision, Writing – original draft, Methodology, Investigation, Conceptualization, Writing – review and editing, Project administration, Funding acquisition, Resources, Validation. KC: Validation, Data curation, Supervision, Methodology, Investigation, Conceptualization, Writing – original draft, Writing – review and editing. JG: Writing – review and editing, Supervision, Resources. SS: Investigation, Validation, Writing – review and editing. LA: Investigation, Writing – review and editing. CB: Writing – review and editing, Investigation. SB: Writing – review and editing, Investigation. MDm: Writing – review and editing, Investigation. MDw: Writing – review and editing, Investigation. RE: Investigation, Writing – review and editing. AE: Investigation, Writing – review and editing. JE: Writing – review and editing, Investigation. DG: Writing – review and editing, Investigation. ScN: Writing – review and editing, Investigation. StN: Writing – review and editing, Investigation. OT: Investigation, Writing – review and editing. CZ: Funding acquisition, Writing – review and editing, Supervision.

Funding

The author(s) declared that financial support was received for this work and/or its publication. This work was undertaken as a senior project in the Electrical, Computer and Systems Engineering (ECSE) Department at Case Western Reserve University under the instruction of Prof. Gregory S. Lee. Funding was provided by the Amateur Radio Digital Communications Foundation (https://www.ardc.net), the Case School of Engineering, the Case Amateur Radio Club W8EDU (https://w8edu.wordpress.com) and the National Science Foundation (NSF AGS-2432824).

Acknowledgements

We acknowledge the staff of CHU, the continental network of volunteers who helped deploy and operate ET units, and the dozens of EQ volunteers who recorded CHU data with their own receivers during the eclipse. We thank the maintainers of the GIRO ionosondes at Millstone Hill, Austin and Alpena for sharing their data through https://giro.uml.edu/. We thank Professor Nathaniel Frissell W2NAF for assistance with data visualization. In Ohio, we thank the members of the Case Amateur Radio Club (W8EDU) who volunteered time to assemble, test, and ship ET units. Equipment for this work was hosted by the research program at CWRU University Farm. Hardware was constructed in the Sears Undergraduate Design Laboratory and think[box]. Incentives were provided by Mitchell's Fine Chocolates and Dewey's Pizza of Cedar Lee. This experiment could only be conducted once in a lifetime. Thank you all for making it possible.

Conflict of interest

Author AG is employed by SpaceX.

The remaining author(s) declared that this work was conducted in the absence of any commercial or financial relationships that could be construed as a potential conflict of interest.

Generative AI statement

The author(s) declared that generative AI was not used in the creation of this manuscript.

Any alternative text (alt text) provided alongside figures in this article has been generated by Frontiers with the support of artificial intelligence and reasonable efforts have been made to ensure accuracy, including review by the authors wherever possible. If you identify any issues, please contact us.

Publisher's note

References

Batchelor, R., Ali, H., Gardner-Vandy, K., Gold, A., MacKinnon, J., and Asher, P. (2021). Reimagining STEM workforce development as a braided river. *Eos* 102. doi:10.1029/2021eo157277

Bonney, R., Ballard, H., Jordan, R., McCallie, E., Phillips, T., Shirk, J., et al. (2009). *Public participation in scientific research: defining the field and assessing its potential for informal science education. a CAISE Inquiry Group report*. Online submission. Available online at: https://files.eric.ed.gov/fulltext/ED519688.pdf.

Boone, A., Rothschild, A., Koo, X., Pfohl, G., Sheehan, A., DiSalvo, B., et al. (2024). Reimagining meaningful data work through citizen science. *Proc. ACM Hum.-Comput. Interact.* 8, 1–26. doi:10.1145/3687049

Cameron, T., Fiori, R., Warrington, E., Stocker, A., Thayaparan, T., and Danskin, D. (2021). Characterization of high latitude radio wave propagation over Canada. *J. Atmos. Solar-Terrestrial Phys.* 219, 105666. doi:10.1016/j.jastp.2021.105666

Collins, K. (2020). 2020 eclipse festival of frequency measurement - 10 Mhz frequency estimation data. doi:10.5281/zenodo.4400117

Collins, K. V. (2023). *Development of a scalable, low-cost meta-instrument for distributed observations of ionospheric variability*. Cleveland, Ohio: Case Western Reserve University. Ph.D. thesis.

Collins, K., Bania-Dobyns, S., Kazdan, D., Vishner, N., and Hennessy, A. (2017). "Radio sloyd: an amateur radio approach to a university-level critical thinking and writing class," in 2017 IEEE Integrated STEM Education Conference (ISEC), 143–149. doi:10.1109/ISECon.2017.7910230

Collins, K., Casente, D., Elia, J., and Mereckis, M. (2021a). 2020 eclipse festival of frequency Measurement: 10 Mhz data. doi:10.5281/zenodo.4959922

Collins, K., Kazdan, D., and Frissell, N. (2021b). Ham radio forms a planet-sized space weather sensor network - eos reprinted in *QST magazine* and elsewhere.

Collins, K., Montare, A., Frissell, N., and Kazdan, D. (2022). Citizen scientists conduct distributed doppler measurement for ionospheric remote sensing. *IEEE Geoscience Remote Sens. Lett.* 19, 1–5. doi:10.1109/lgrs.2021.3063361

Collins, K., Gibbons, J., Frissell, N., Montare, A., Kazdan, D., Kalmbach, D., et al. (2023). Crowdsourced Doppler measurements of time standard stations demonstrating ionospheric variability. *Earth Syst. Sci. Data* 15, 1403–1418. doi:10.5194/essd-15-1403-2023

Cooke, N. J., and Hilton, M. L. (2015). *Enhancing the effectiveness of team science*. Washington, DC: The National Academies Press. doi:10.17226/19007

[Dataset] Kerkwijk, M. V., Tollerud, E., Woillez, J., Robitaille, T., Bray, E. M., Valentino, A., et al.(2020). Liberfa/pyerfa v1.7.0. doi:10.5281/ZENODO.3940699

Esmaeili-Karnawah, A., Fallah, R., Khorashadizadeh, S. M., and Niknam, A. R. (2024). Propagation characteristics analysis of high-frequency radio waves in the lower ionosphere layers. *Heliyon* 10, e40963. doi:10.1016/j.heliyon.2024.e40963

Espenak, F. (2014). Eclipse predictions. Available online at: www.eclipsewise.com.

Frissell, N. (2017). w2naf/eclipse_calculator v1.0. doi:10.5281/zenodo.1120440

Frissell, N. A., Katz, J. D., Gunning, S. W., Vega, J. S., Gerrard, A. J., Earle, G. D., et al. (2018). Modeling amateur radio soundings of the ionospheric response to the 2017 great American eclipse. *Geophys. Res. Lett.* 45, 4665–4674. doi:10.1029/2018GL077324

Frissell, N. A., Ackermann, J. R., Alexander, J. N., Benedict, R. L., Blackwell, W. C., Boedicker, R. K., et al. (2023). Heliophysics and amateur radio: citizen science collaborations for atmospheric, ionospheric, and space physics research and operations. *Front. Astronomy Space Sci.* 10, 10–2023. doi:10.3389/fspas.2023.1184171

Garvin, D. A. (1987). Competing on the eight dimensions of quality. *Harv. Bus. Rev.*

Gibbons, J. (2024). Grape 2 - the finalized version (Cleveland, OH: HamSCI workshop)

Gibbons, J., Collins, K., Kazdan, D., and Frissell, N. (2022). Grape version 1: first prototype of the low-cost personal space weather station receiver. *HardwareX* 11, e00289. doi:10.1016/j.ohx.2022.e00289

Goodman, A., Usis, M., Schwartz, L., and Collins, K. (2024a). CHU time of flight data. *8 April 2024 eclipse - stations*. doi:10.5281/zenodo.14257092

Goodman, A., Usis, M., Schwartz, L., Kazdan, D., and Gibbons, J. (2024b). ET station setup instructions for CHU measurement, April 8, 2024 solar eclipse. doi:10.5281/zenodo.13293307

Goodman, A., Usis, M., Schwartz, L., Trautmann, C., Harder, R., St. Columbia, J., et al. (2025). CHU eclipse data — Audio recordings (EQ). doi:10.5281/zenodo.17069914

Hughes, P. (2024). *A century of weather service: a history of the birth and growth of the National Weather Service, 1870-1970*. London: Routledge. doi:10.4324/9781003522195

Ioannidis, J. P. A., Fanelli, D., Dunne, D. D., and Goodman, S. N. (2015). Meta-research: evaluation and improvement of research methods and practices. *PLOS Biol.* 13, e1002264. doi:10.1371/journal.pbio.1002264

Kazdan, D. (2024). The 2024 North American solar eclipse: W8EDU, HamSCI and the CHU along-path measurement project. *Can. Amateur* 52, 10–12.

Lane, A. P., and Walsh, F. X. (1925). The effects of the eclipse on radio. *Sci. Am.* 132, 224–226. doi:10.1038/scientificamerican0425-224

Ledvina, V., Brandt, L., MacDonald, E., Frissell, N., Anderson, J., Chen, T. Y., et al. (2023). Agile collaboration: citizen science as a transdisciplinary approach to heliophysics. *Front. Astronomy Space Sci.* 10, 10–2023. doi:10.3389/fspas.2023.1165254

Lyubovtseva, Y. S., Gvishiani, A. D., Soloviev, A. A., Samokhina, O. O., and Krasnoperov, R. I. (2020). Sixtieth anniversary of the International Geophysical Year (1957–2017) – contribution of the Soviet Union. *Hist. Geo- Space Sci.* 11, 157–171. doi:10.5194/hgss-11-157-2020

Mason, B. M., Mesaglio, T., Barratt Heitmann, J., Chandler, M., Chowdhury, S., Gorta, S. B. Z., et al. (2025). iNaturalist accelerates biodiversity research. *BioScience* 75, 953–965. doi:10.1093/biosci/biaf104

McCray, W. P. (2021). *Keep watching the skies: the story of Operation Moonwatch and the dawn of the space age*. Princeton, NJ: Princeton University Press.

Meehan, T. D., Michel, N. L., and Rue, H. (2019). Spatial modeling of Audubon Christmas bird counts reveals fine-scale patterns and drivers of relative abundance trends. *Ecosphere* 10, e02707. doi:10.1002/ecs2.2707

Meisel, D. D., Duke, B., Aguglia, R. C., and Goldblatt, N. R. (1976). Solar eclipse effects on HF and VLF propagation. *J. Atmos. Terr. Phys.* 38, 495–502. doi:10.1016/0021-9169(76)90006-4

Mesquita, R. L. A., Barnes, R., Gjerloev, J., Eisape, A., Mosavi, N., and Eidson, R. (2025). Eclipse-induced geomagnetic signatures: the 2024 EZIE-mag citizen science campaign contribution to the heliophysics big year. *Front. Astronomy Space Sci.* 12, 12–2025. doi:10.3389/fspas.2025.1601396

Munn, O. (1924). Help us study the solar eclipse. *Sci. Am.* 131, 312.

Nanda, S., and Treseler, Z. (2024). Case amateur radio club gains national attention for eclipse research. *Observer*. Available online at: https://observer.case.edu/Case-Amateur-Radio-Club-gains-national-attention-for-eclipse-research.

National Academies of Sciences, E. and Medicine (2018). *Learning through citizen science: enhancing opportunities by design*. Washington, DC: The National Academies Press. doi:10.17226/25183

National Research Council (2012). *Lessons and legacies of international polar year 2007-2008*. Washington, DC: The National Academies Press. doi:10.17226/13321

NOAA Space Weather Prediction Center (2024). Planetary K-index. Available online at: https://www.swpc.noaa.gov/products/planetary-k-index.

Pearce, J. M. (2012). Building research equipment with free, open-source hardware. *Science* 337, 1303–1304. doi:10.1126/science.1228183

Poole, I. (1999). Radio waves and the ionosphere. *QST Mag.*

Project Management Institute (2004). *A guide to the project management body of knowledge (PMBOK)*. 3 edn. Newton Square, PA: Project Management Institute.

Price-Whelan, A. M., Lim, P. L., Earl, N., Starkman, N., Bradley, L., Shupe, D. L., et al. (2022). The astropy project: sustaining and growing a community-oriented open-source project and the latest major release (v5.0) of the core package. *Astrophysical J.* 935, 167. doi:10.3847/1538-4357/ac7c74

Radicella, S. M., and Migoya-Orué, Y. O. (2021). *GNSS-derived data for the study of the ionosphere*. Elsevier, 221–239. doi:10.1016/b978-0-12-818617-6.00020-2

Reinisch, B. W., and Galkin, I. A. (2011). Global ionospheric radio observatory (GIRO). *Earth, Planets Space* 63, 377–381. doi:10.5047/eps.2011.03.001

Usis, M. (2024). Gps-synchronized recordings of 10 mhz during October 2, 2024 eclipse from tortel, aysén, Chile. PhD thesis. doi:10.5281/zenodo.14004514

Usis, M. (2025). *Design and deployment of a distributed data collection system for HF radio measurements during the great North American eclipse of 2024*. Cleveland, Ohio: Case Western Reserve University. Master's thesis.

Weiss, J., Smythe, W., and Lu, W. (2005). "Science traceability," in 2005 IEEE Aerospace Conference, 292–299. doi:10.1109/AERO.2005.1559323

Yeang, C.-P. (2013). *Probing the sky with radio waves: from wireless technology to the development of atmospheric science*. University of Chicago Press. doi:10.7208/chicago/9780226034812.001.0001

Zhang, S.-R., Erickson, P. J., Goncharenko, L. P., Coster, A. J., and Frissell, N. A. (2017). Monitoring the geospace response to the great American solar eclipse on 21 August 2017. *Earth Planet. Phys.* 1, 72–76. doi:10.26464/epp2017011